Thermal Conductivity of Superconducting Th and Th-Gd Alloys*

R. L. CAPPELLETT† AND D. K. FINNEMORE
Institute for Atomic Research and Department of Physics, Iowa State University, Ames, Iowa 50010
(Received 16 July 1969)

Thermal conductivity measurements are reported for both the normal and superconducting states of pure Th and Th-Gd alloys. The pure Th results show significant deviations from the Bardeen-Rickayzen-Tewordt theory, but these deviations are consistent with the observed anisotropy of the energy gap. Measurements for the Th-Gd alloys agree well with the theory of Ambegaokar and Griffin for paramagnetic-impurity-doped superconductors.

INTRODUCTION

THE equilibrium properties of superconductors containing magnetic impurities have been studied in considerable detail,[1] but the transport properties have received much less attention. Detailed theoretical work on this problem has been carried out by Ambegaokar and Griffin[2] and by Gruenberg,[3] but as yet the only experimental work has dealt with related problems for thin films and surface phenomena. Experiments by Mochel and Parks[4] and by Smith and Ginsberg[5] confirmed the general features of the transport theory for the case of nonmagnetic impurity-doped thin films in an external field and another experiment by Deutscher, Lindenfeld, and McConnell[6] confirmed the theory for the proximity effect. Although these problems differ from the magnetic impurity case in some ways, there is a strong formal resemblance.[7] The object of this work is to study the transport properties of bulk superconductors doped with paramagnetic impurities.

In this paper we report thermal conductivity measurements as a function of temperature and impurity concentration for superconducting Th doped with the magnetic impurity Gd. This alloy system is especially well suited for these studies because pure Th is a weak coupling superconductor, the magnetic impurities are paramagnetic, and the alloys are type-I superconductors over most of the range of interest. In addition, the equilibrium properties have been studied in detail.[8]

EXPERIMENT

Sample Preparation

Both of the Th-Gd samples reported here are the same samples used for the earlier critical-field work,[8] and a detailed account of their preparation was given in that publication. The pure-Th samples used for the critical-field work, unfortunately, was not suitable for these transport measurements because the resistivity was so low that the scattering of electrons by phonons would be an important factor. It is much easier to unravel thermal conductivity results in metals if the electrons are scattered predominantly by impurities. Hence we selected a "nominally" pure Th sample with sufficient nonmagnetic impurities to ensure that the scattering of electrons by phonons would not be important. This sample was prepared in exactly the same way as the Th-Gd alloys.

Thermometry

A temperature scale was established by calibrating a Ge resistance thermometer in a separate experiment. He^4 vapor pressures were used as the primary standard in the region above 1.2°K, and below this temperature the susceptibility of chrome methylamine alum was used as the standard. Corrections to the Curie law for the chrome methylamine alum were taken from the theory of Hebb and Purcell as described previously.[9] Precision in these temperature measurements is better than 0.001°K but there may be larger systematic errors due to the uncertainties in the corrections to the Curie law for the salt susceptibility. The Ge resistor was then used to calibrate the Speer C resistors on each thermal conductivity run.

Experimental Equipment

Temperatures from 4.2 to 0.3°K were maintained with a conventional He^3 refrigerator shown in Fig. 1. A He^4 evaporator (A), a He^3 evaporator (B), and the thermal conductivity apparatus were all enclosed in a common vacuum space which was submerged in a He^4 bath at 4.2°K. Under ordinary operating conditions,

* Work was performed in the Ames Laboratory of the U. S. Atomic Energy Commission, Contribution No. 2536.

† Present address: Department of Physics, Ohio University, Athens, Ohio.

[1] M. A. Woolf and F. Reif, Phys. Rev. **137**, A557 (1965).

[2] V. Ambegaokar and A. Griffin, Phys. Rev. **137**, A1151 (1965).

[3] L. Gruenberg, Phys. Rev. **138**, A78 (1965).

[4] J. M. Mochel and R. D. Parks, Phys. Rev. Letters **16**, 1156 (1966).

[5] J. E. Smith, Jr., and D. M. Ginsberg, Phys. Rev. **167**, 345 (1968).

G. Deutscher, P. Lindenfield, and R. D. McConnell, Phys. Rev. Letters **21**, 79 (1968).

[7] K. Maki, Progr. Theoret. Phys. (Kyoto) **31**, 731 (1965); K. Maki and P. Fulde, Phys. Rev. **140**, A1586 (1965); P. G. de Gennes, Phys. Condensed Matter **3**, 79 (1964).

[8] W. R. Decker and D. K. Finnemore, Phys. Rev. **172**, 430 (1968).

[9] D. K. Finnemore and D. E. Mapother, Phys. Rev. **140**, A507 (1965).

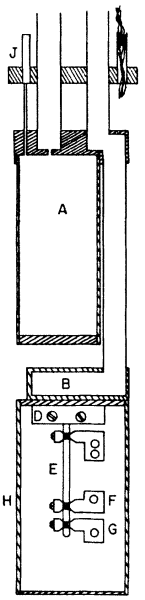

FIG. 1. Cryostat assembly. A is the He^4 reservoir; B is the He^3 reservoir; C is the epoxy seal; D is the cold sink; E is the sample; F is the high-temperature thermometer; G is the heater; H is the heat shield; and J is the He^4 needle valve.

the He^4 evaporator was filled from the surrounding bath through a needle valve (J) and the He^3 evaporator was filled with approximately 1 liquid cm^3 of He^3 by letting gas into the main pumping line. Once these reservoirs were filled, the refrigerator was set for a full day of operation. Temperature control was accomplished by throttling the He^3 pumping speed to give a few μW of cooling power at the temperature desired and this cooling power was then automatically balanced by a thermometer controlled heater. Drifting thermal emf's were the main problem in temperature control, but by packaging most of the low-level circuitry in an adiabatic environment and by the use of continuous leads and low-thermal solder, the drift rate was reduced to 0.5 μV/h. Temperatures below 1°K could then be controlled to 10^{-5}°K for periods up to 1 h.

Heat leaks into the sample region were reduced by a number of precautions. Light traps were used to block the radiation from room temperature. All electrical leads passed directly through the He^4 bath and entered the vacuum space through an epoxy seal. These leads were then thermally anchored to the He^4 evaporator, and the He^3 evaporator, and the sample clamps with GE-7031 varnish. All leads between the last thermal sink and the thermometers consisted of 5-in. lengths of No. 44 Manganin wire. Calculations indicate that the error in the thermal conductivity measurements due to heat conduction and heat generated in the leads was never greater than 0.1%. One voltage lead to the sample heater was connected to the thermal sink end. This arrangement accounts for the joule heating in the lead wires to a few parts in 10^4.

The sample clamps (F) shown in Fig. 1 were made from free-machining Te-Cu. A thin coat of Apiezon-N grease was applied where contact was made to the sample. Each of the resistors was also greased and fitted into a hole in the appropriate clamp. As a further precaution, each electrical lead to the thermometers was thermally anchored to the clamp by soldering the leads to Cu sheets which were then glued, over electrically insulating cigarette paper, to the clamp with GE-7031 varnish. Such anchoring is especially important for the Ge thermometer because the encapsulating case is not in good thermal contact with the Ge.

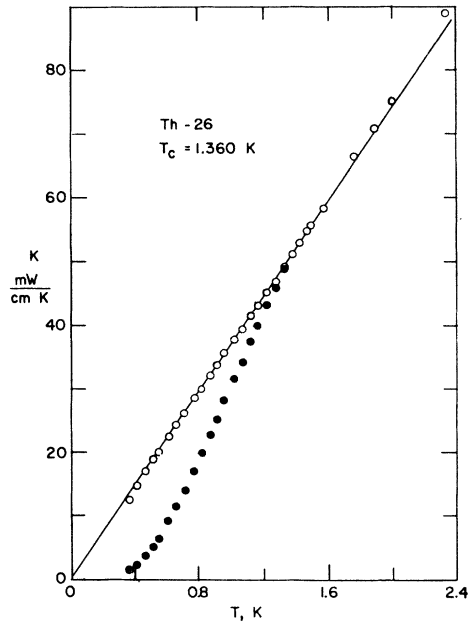

FIG. 2. Thermal conductivity of a nominally-pure-Th sample with a resistivity ratio of 26. Open circles are normal-state data, and the solid circles are superconducting-state data.

A Guildline potentiometer and galvanometer amplifier with a sensitivity of 10^{-8} V was used to measure voltages. The thermometer measuring currents, usually 1 μA, were supplied by Hg cells. The precision in measuring the temperature drop across the sample was better than 0.1%.

Experimental Procedure

A steady-state method was used to measure the thermal conductivity, K. Heater power P_h was applied at the lower end of the sample and the resulting temperature gradient was measured by the Ge resistor GR at the cold end and a Speer carbon resistor at the hot end R_h. Another Speer carbon resistor R_c, which had nearly the same resistance temperature curve as R_h, was placed at the cold end to facilitate the temperature gradient ΔT determination. In the course of a thermal-conductivity measurement, GR and R_c were held fixed as P_h was increased and the difference $R_c - R_h = \Delta R$ was measured directly by placing R_c and R_h in two

arms of the Wheatstone bridge. This direct measurement of ΔR gives much better precision than the alternate method of measuring R_c and R_h separately and subtracting these two quantities. Both methods were tried; the former gave a precision four times better. R_h was then calibrated against GR with zero heater power at each thermal conductivity point and this calibration was then fit to a function of the form

$$\ln T=\sum_{n=1}^{n=6} Q_n \ln(R_h)^{n-1}. \quad (1)$$

The fit to this equation is good to 3 mdeg over the entire range. The temperature of the cold end T_m was determined from GR. The temperature increment ΔT was determined from the measured value of ΔR and the smooth curve, Eq. (1); and the average temperature of the sample T_s was taken to be

$$T_s=T_m+\tfrac{1}{2}\Delta T.$$

The length l and cross-sectional area A of the sample

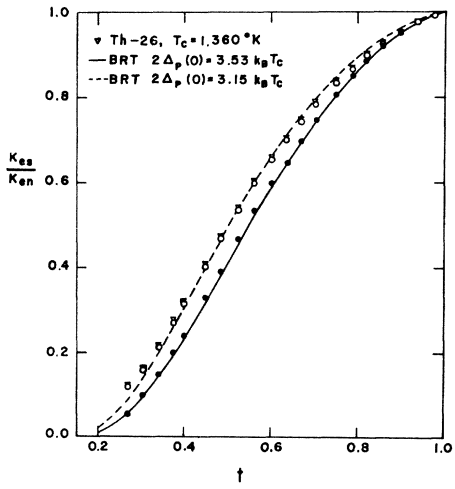

FIG. 3. Ratio of the superconducting to normal-state electronic thermal conductivity of thorium. Triangles, raw data, assume no phonon contribution. Open circles assume a dislocation scattering-limited phonon contribution, and the solid circles assume both dislocation and electron scattering of the phonons.

were determined with a traveling microscope and micrometer. The thermal conductivity is then given by

$$K(T_s)=(l/A)P_h/\Delta T.$$

ΔT was kept small enough in each measurement ($\Delta T/T\sim 0.05$), so that this equation is estimated to represent the thermal conductivity to within 0.5%.

To measure the magnetic-field dependence of the thermal conductivity, P_h is adjusted to maintain constant ΔT during the superconducting to normal phase transition. $K(H)/K(0)$ is then given by the ratio of the respective heater powers, and errors in determining ΔT cancel. Hence, the ratio of the superconducting thermal conductivity K_s to the normal thermal conductivity K_n is more accurately measured than either K_s or K_n.

RESULTS AND DISCUSSION

Pure Th

Figure 2 shows the thermal conductivity data for pure Th in both the superconducting (solid circles) and normal (open circles) states. At low temperatures, the normal-state conductivity has nearly a linear temperature dependence, as would be expected if the electrons were the dominant heat carrier and the electronic mean free path were limited by impurity scattering. The Lorenz number derived from these data, and the measured electrical resistivity $\rho=0.625$ $\mu\Omega$ cm is 2.3×10^{-8} W Ω/K^2, in good agreement with the elementary theory. Uncertainty in this number arises primarily in the determination of the length-to-area ratio for the sample. Above 1.6°K, K_n data show a slight upward curvature, indicating a small phonon contribution, but these data do not cover a wide enough temperature range to clearly establish the temperature dependence of the phonon term. Thermal conductivity measurements on similar Th samples at higher temperatures[10] also confirm that the lattice term should be small. For this particular specimen, the sample size (0.1 mm) and the grain size (0.01 mm) are large, so we have assumed that dislocations and normal electrons are the dominant scattering centers for phonons. Both of these mechanisms are expected[11] to give phonon conductivities which vary as T^2, so the K_n data have

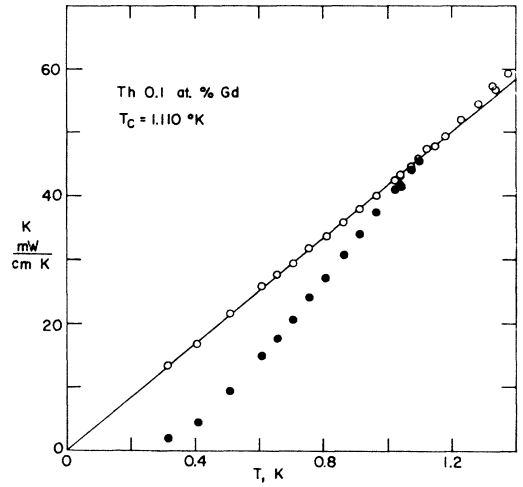

FIG. 4. Thermal conductivity of Th 0.1 at.% Gd. The solid line is the Wiedemann-Franz law for a Lorenz number of 2.5×10^{-8} W Ω K^{-2}.

[10] H. Schettler, Ph.D. thesis, Iowa State University, Ames, Iowa, 1969 (unpublished).

[11] G. Slack, Phys. Rev. **105**, 832 (1957); J. M. Ziman, *Electrons and Phonons* (Oxford University Press, London, 1962).

been fit to an equation of the form

$$K_n = AT + BT^2,$$

where A and B are constants. AT is then interpreted as the normal electronic conductivity (K_{en}) and BT^2 is interpreted as the normal lattice conductivity (K_{gn}). A least-squares fit to the data gives $A = 36.57$ mW/cm K^2 and $B = 0.514$ mW/cm K^3 so it appears that K_{en} dominates for temperatures below 1.4°K.

Transitions from the normal to the superconducting state are sharp and agree with the magnetization measurements of Decker.[8] All the normal-state data reported here were taken in fields of 200 Oe or less, so that there would be no difficulty from the magnetoresistance of the C and Ge resistors. The transition temperature of 1.360°K, which was determined from the measured resistivity and a curve of the depression of T_c,[12] is in good agreement with the extrapolation of the thermal conductivity data.

A comparison of the superconducting-state data with the theory is somewhat complicated because the phonon conductivity K_{gs} is not necessarily as small as it is in the normal state. If dislocation scattering completely dominates the lattice conductivity, then the phonon term will be the same in both the superconducting and normal states. If, however, electron scattering of phonons is also important, then this contribution to the conductivity is expected to be larger by the R_g factor given by the theory of Bardeen, Rickayzen, and Tewordt (BRT).[13] There is no way to reliably separate these contributions, so a unique analysis of the results is impossible. Hence the procedure adopted here is to analyze the data for two extreme cases in order to designate the region where the electronic conductivity lies.

An upper bound on the superconducting electronic conductivity K_{es} would be set by the assumption that the phonon conductivity is completely dominated by dislocation scattering. For this case, $K_{gs} = K_{gn} = BT^2$ and the superconducting electronic conductivity can be obtained by the subtraction

$$K_{es} = K_s - BT^2.$$

A plot of the resulting data in the form K_{es}/K_{en} is shown by the open circles of Fig. 3. For this sample, the phonon conductivity is so small that its subtraction makes very little difference. We have $K_{es}/K_{en} = K_s/K_n$ to an accuracy of better than 1%. The K_s/K_n data are shown as the open triangles for comparison. These data all lie well above the BRT predictions,[13] but this sort of behavior is to be expected for a superconductor with an anisotropic energy gap. At present, the values of the energy gap in various directions are not known, but recent measurements[12] of the depression of T_c in Th-C alloys indicate a mean-square-gap anisotropy of 0.021. This means that the gap varies from about 3.0 to $4.0kT_c$ for different directions in the crystal. As was discussed by Burkbuchler, Markowitz, and Reynolds,[14]

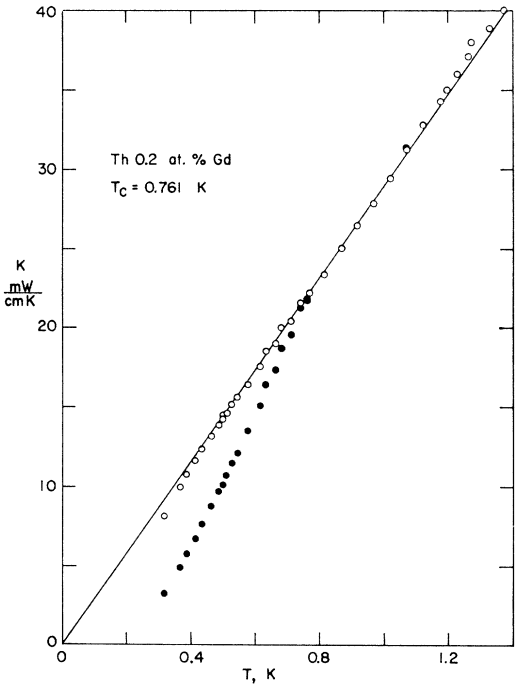

FIG. 5. Thermal conductivity of Th 0.2 at.% Gd. The solid line is the Wiedemann-Franz law for a Lorenz number of 2.6×10^{-8} W Ω K^{-2}.

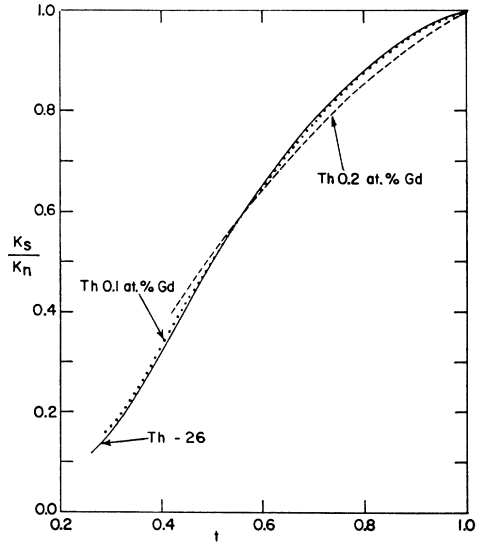

FIG. 6. Comparison of pure Th with the Th-Gd alloys. At high temperatures the alloy data lie below pure Th, and at low temperatures they lie above the pure-Th data.

[12] J. W. Anderson, D. T. Peterson, and D. K. Finnemore, Phys. Rev. **179**, 472 (1969).

[13] J. Bardeen, G. Rickayzen, and L. Tewordt, Phys. Rev. **113**, 982 (1959).

[14] F. V. Burkbuchler, D. Markowitz, and C. A. Reynolds, Phys. Rev. **175**, 556 (1968).

those portions of the Fermi surface with small gap tend to dominate the thermal conductivity at low temperatures, so one would expect K_{es}/K_{en} to lie above the BRT curve. To make a qualitative comparison with the data, we have scaled the BCS energy gap by various constant factors and have calculated a family of thermal conductivity curves within the BRT framework. The best fit, shown by the dashed line of Fig. 3, occurs for $2\Delta_p(0)=3.15kT_c$. This isotropic-gap description overestimates the thermal conductivity at high reduced temperatures and underestimates it at low

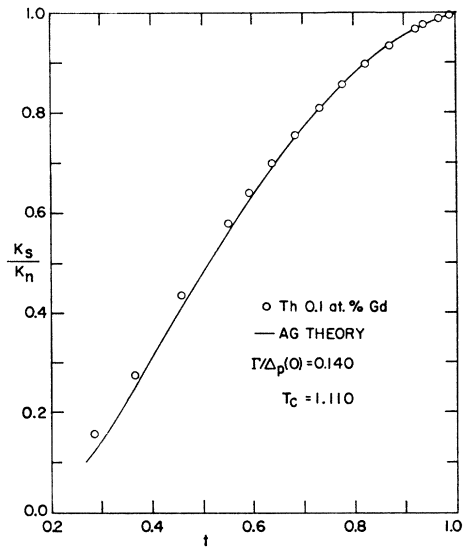

FIG. 7. Comparison of Th 0.1 at.% Gd data with AG theory.

temperatures. Such behavior is not surprising since gap anisotropy would be expected to produce a stronger effect at low temperatures where regions of small gap are relatively more heavily populated with thermal excitations. A more detailed analysis must await direct measurements of the gap anisotropy.

A lower bound for K_{es} at low temperature is probably set by the BRT thermal conductivity.[13] Ordinarily, a superconductor with an average energy gap of $3.53kT_c$ [8] and a mean-squares anisotropy of 0.021 [12] would be expected to have an electronic conductivity somewhat larger than the theory.[13] To gain further insight into these results, we have made several assumptions about the various contributions to the conductivity and have calculated a lower bound curve shown by the solid dots of Fig. 3. The assumptions are: (1) The phonon conductivity limited by dislocation scattering is the same in the superconducting and normal states. (2) The phonon conductivity limited by electron scattering in the superconducting state is related to that in the normal state by the BRT factor R_g. (3) The two-phonon resistivity terms are additive. With these assumptions, one can force the K_{es} data to fit BRT at one temperature and then calculate K_{es} for all other temperatures. The

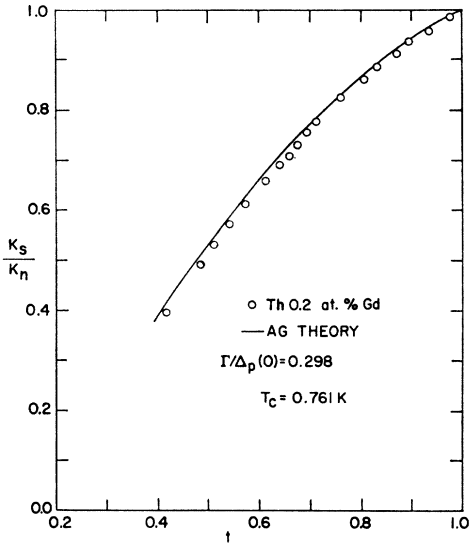

FIG. 8. Comparison of Th 0.2 at.% Gd data with AG theory.

solid data of Fig. 3 represent such a calculation where the data have been forced to fit BRT at the lowest temperature $T=0.367$°K. At all other temperatures the fit to BRT is rather good, although the data lie somewhat above the theory. The important point here is that the K_{es}/K_{en} data lie above the BRT theory for reasonable assumptions about the phonon contribution.

Th-Gd Alloys

Figures 4 and 5 show the superconducting and normal-state data for Th 0.10 at.% Gd and Th 0.20 at.% Gd. The solid lines on each of these figures represent the Wiedemann-Franz law contributions for Lorenz numbers of 2.5×10^{-8} and 2.6×10^{-8} W Ω K^{-2}, respectively. Again, the uncertainties arise primarily from the determination of the length-to-area ratio.

The small upward deviations from linear behavior indicate that the phonon contribution is about the same size as in the pure-Th sample. In the analysis of these alloy data we have used the pure-Th results as a guide to proper handling of the phonon terms. The upper bound curve of Fig. 3 (open circles) which assumes no phonon contribution seems to agree with the measured anisotropy of the energy gap,[12] so we have analyzed the alloy data with this assumption. The K_s/K_n data differ from the upper bound K_{es}/K_{en} data by less than 1%, so the data are all cast as K_s/K_n. For each of the alloy samples, T_c was taken from the critical-field work of Decker.[8]

K_s/K_n data presented in Fig. 6 show qualitative agreement with the main features of the Ambegaokar-Griffin (AG)[2] theory. Near T_c, the data for the alloy samples lie below the pure-metal (Th-26) curve, and at lower temperatures the curves cross over and the alloy data show a higher thermal conductivity. This agree-

ment is not too surprising for this particular alloy system because the magnetic scattering time (10^{-11} sec) is much longer than the nonmagnetic scattering time (10^{-14} sec), and we know from susceptibility measurements that the Gd ions are paramagnetic. These are exactly the conditions for the application of the AG theory. No attempt is made to compare with the Gruenberg theory,[3] because the spin-scattering time is too long.

In order to make a direct quantitative comparison with the theory, we used the measured value of the alloy transition temperature T_c and the pure-metal transition temperature T_{cp} in conjunction with the theory to calculate the lifetime broadening, the order parameter, and the thermal conductivity. Details of this sort of calculation are given elsewhere.[8] Results for both the theory (solid line) and experiment (open circle) are shown in Figs. 7 and 8. This must be considered to be very good agreement providing one can assume that the addition of magnetic impurity does not change the phonon contribution.

CONCLUSION

From this work and the earlier equilibrium measurements[8] we conclude that the Abrikosov-Gorkov theory[15] (and its extension to transport properties by Ambegaokar and Griffin) of superconductors containing paramagnetic impurities describes both the equilibrium and transport properties of Th-Gd alloys to a very high accuracy. Not only is the theory qualitatively correct, but it is quantitatively correct to a few percent.

[15] A. A. Abrikosov and L. P. Gorkov, Zh. Eksperim. i Teor. Fiz. **39**, 178 (1960) [English transl.: Soviet Phys.—JETP **12**, 1243 (1961)].

PHYSICAL REVIEW VOLUME 188, NUMBER 2 10 DECEMBER 1969

Elastic Properties of Superconductors: Nb, V, and Ta†

G. W. GOODRICH* AND J. N. LANGE
Department of Physics, Oklahoma State University, Stillwater, Oklahoma 74074

(Received 17 July 1969)

The magnetic field dependence of Young's modulus of type-I and type-II superconductors is used to study the properties of the intermediate and mixed states. The density and separation of vortices in the mixed state are computed from the observed field dependence of the elasticity by use of a model which allows the vortex to expand. A residual stiffness associated with trapped flux is observed to decrease at lower temperatures as a result of reduced pinning forces acting on the vortices. The pinning forces appear to be associated with more than elastic coupling done to the imperfections. The largest total change in stiffness due to the superconducting transition is associated with the longest normal-electron mean free path. Shielding of the lattice initeractions in the superconductng state appears to be more effective the longer the coherence of the superconducting pairs between scatterings. Use of elastic measurements as a means of determining bulk characteristics of the superconductor is found to be quite accurate for materials with low acoustic losses. Anisotropies in the bulk critical fields of niobium are determined simultaneously with the magnetization.

INTRODUCTION

THE elastic properties of solids are modified by the transition to the superconducting state. An early success of the Bardeen-Cooper-Schriefer theory of superconductivity resulted from its ability to predict the temperature dependence of the ultrasonic attenuation, which has since become a standard technique to determine energy gaps of superconducting solids. Changes in the stiffness of a solid entering the superconducting state are much smaller than those of the attenuation. Experimental techniques of high accuracy are needed to observe the transition. Observations of these elastic changes were first made in tin.[1–3] Ensuing work by Alers and Waldorf[4,5] also considered type-II superconductors. Recent investigations by Kramer and Bauer have determined both the temperature[6] and magnetic field[7] dependence of the elasticity in superconducting Nb.

† Work supported by the National Science Foundation.
* Submitted in partial fulfillment of requirements for the Ph.D. degree at the Oklahoma State University.

[1] J. K. Landaver, Phys. Rev. **96**, 296 (1954).
[2] B. Welber and S. L. Quimby, Acta Met. **6**, 351 (1958).
[3] D. F. Gibbins and C. A. Renton, Phys. Rev. **114**, 1257 (1969).
[4] G. A. Alers and D. L. Waldorf, Phys. Rev. Letters **6**, 677 (1961).
[5] G. A. Alers and D. L. Waldorf, IBM J. Res. Develop. **6**, 89 (1962).
[6] E. J. Kramer and C. L. Bauer, Phys. Rev. **163**, 407 (1967).
[7] E. J. Kramer and C. L. Bauer, Phys. Status Solidi **22**, 199 (1967).